Published December 1, 1994

Regulated Internalization of Caveolae

Robert G. Parton, Brigitte Joggerst, and Kai Simons

European Molecular Biology Laboratory, D69012 Heidelberg, Germany

Abstract. Caveolae are specialized invaginations of the plasma membrane which have been proposed to play a role in diverse cellular processes such as endocytosis and signal transduction. We have developed an assay to determine the fraction of internal versus plasma membrane caveolae. The GPI-anchored protein, alkaline phosphatase, was clustered in caveolae after antibody-induced crosslinking at low temperature and then, after various treatments, the relative amount of alkaline phosphatase on the cell surface was determined. Using this assay we were able to show a time- and temperature-dependent decrease in cell-surface alkaline phosphatase activity which was dependent on antibody-induced clustering. The decrease in cell surface alkaline phosphatase activity was greatly accelerated by the phosphatase inhibitor, okadaic acid, but not by a protein kinase C activator. Internalization of clustered alkaline phosphatase in the presence or absence of okadaic acid was blocked by cytochalasin D and by the kinase inhibitor staurosporine. Electron microscopy confirmed that okadaic acid induced removal of caveolae from the cell surface. In the presence of hypertonic medium this was followed by the redistribution of groups of caveolae to the center of the cell close to the microtubule-organizing center. This process was reversible, blocked by cytochalasin D, and the centralization of the caveolar clusters was shown to be dependent on an intact microtubule network. Although the exact mechanism of internalization remains unknown, the results show that caveolae are dynamic structures which can be internalized into the cell. This process may be regulated by kinase activity and require an intact actin network.

CAVEOLAE or plasmalemmal vesicles are a characteristic feature of the plasma membrane of many mammalian cell types (for review see Severs, 1988). Morphologically, caveolae are 50–60-nm invaginations of the plasma membrane with a characteristic flask shape. Unlike clathrin-coated pits, caveolae have no clearly defined coat by transmission electron microscopy of conventionally prepared specimens. However, under certain conditions a characteristic spiral coat is visible on the cytoplasmic side of the caveolae (Peters et al., 1985) consisting in part of the integral membrane protein VIP21/caveolin (Rothberg et al., 1992; Dupree et al., 1993; Kurzchalia et al., 1994). A number of molecules have now been localized to caveolae including a plasma membrane Ca-ATPase and an IP_3-receptor-like protein (Fujimoto, 1993; Fujimoto et al., 1993). Other molecules have been shown to associate with caveolae under certain conditions. For example, GPI-anchored proteins (Mayor et al., 1994), VIP-36 (Fiedler et al., 1994), and the β-adrenergic receptor (Raposo et al., 1989; Dupree et al., 1993) are concentrated in caveolae after cell surface labeling with antibodies. Other molecules postulated to be associated with caveolae include tyrosine kinases and kinase substrates which are enriched in VIP21/caveolin-containing detergent-insoluble complexes (Sargiacomo et al., 1993). However, it is not yet clear to what extent these molecules are associated with caveolae in vivo; for example, VIP-36 and many GPI-anchored proteins are associated with these detergent-insoluble complexes but do not appear to be significantly enriched in caveolae under physiological conditions (Fiedler et al., 1994; Mayor et al., 1994). Caveolae may also have a distinct lipid composition. The ganglioside GM1 has been shown to be enriched in caveolae (Parton, 1994) and cholesterol is essential for their structure and function (Rothberg et al., 1990*a*, 1992; Chang et al., 1992).

A number of different functions have been proposed for caveolae including signal transduction (Lisanti et al., 1994*a*), potocytosis (Anderson, 1993), calcium regulation or signaling (Fujimoto, 1993; Fujimoto et al., 1993), and non-clathrin-dependent endocytosis and transcytosis (Montesano et al., 1982; Milici et al., 1987; Tran et al., 1987). Early studies suggested a role for caveolae or plasmalemmal vesicles in endothelial cells in transport across the monolayer (Ghitescu et al., 1986; Milici et al., 1987; Simionescu and Simionescu, 1991). However, other studies concluded that in endothelial cells most, if not all, caveolae were connected to the cell surface and were not free vesicles (Bundgaard, 1983; Bundgaard et al., 1983). Studies of cultured cells showed that uncoated invaginations were able to inter-

Address all correspondence to Dr. R. G. Parton, EMBL, Meyerhofstr. 1, D69012 Heidelberg, Germany. Fax: 49 6221-387.306.

Published December 1, 1994

nalize toxin-gold conjugates (Montesano et al., 1982; Tran et al., 1987). These invaginations were subsequently shown to be caveolae as defined by VIP21/caveolin labeling (Parton, 1994). However, others have argued against any role for caveolae in endocytosis (Van Deurs et al., 1993). The role of caveolae in potocytosis (Anderson et al., 1992; Anderson, 1993) has also been questioned by the finding that GPI-anchored proteins are present in similar concentrations in clathrin-coated pits and caveolae (Mayor et al., 1994). We have therefore developed an assay to examine whether caveolae remain attached to the cell surface and to examine conditions which might stimulate their internalization. Here we show that a small fraction of plasma membrane caveolae do lose their connection to the cell surface and that this is regulated by kinase activity.

Materials and Methods

Cells, Antibodies, and Other Reagents

A431 cells and MDCK cells were cultured as previously described (Dupree et al., 1993). A431 cells were plated 18–24 h before each experiment and were used at 60–80% confluency. MDCK cells were grown on glass coverslips for 2–3 d until confluent. Affinity-purified antibodies to a peptide corresponding to the NH_2-terminus of VIP21/caveolin (anti-VIP21N/caveolin) were characterized previously (Dupree et al., 1993). Cholera toxin-binding subunit (CT-B)[1] and CT-B conjugated to horseradish peroxidase (CT-B–HRP) were purchased from Sigma Chem. Co. (St. Louis, MO). CT-B adsorbed to 10 or 14 nm gold (CT-B–gold) was prepared exactly as described previously (Parton, 1994). Antiserum to cholera toxin was a kind gift from Dr. D. R. Critchley (Department of Biochemistry, University of Leicester, England). Cytochalasin D (CytD), nocodazole, phorbol 12-myristate 13-acetate (PMA), *p*-nitrophenyl phosphate, and staurosporine were purchased from Sigma and okadaic acid (OA) and genistein from Gibco (Paisley, Scotland). Monoclonal antibodies to human placental alkaline phosphatase were purchased from Dako (Glostrup, Denmark) and Zymed (San Francisco, CA).

Surface Labeling of Cells for Morphological Experiments

Labeling with Antibodies to Alkaline Phosphatase. A431 cells were washed in DMEM/25 mM Hepes and then incubated sequentially with mouse monoclonal antibodies to human placental alkaline phosphatase (Dako or Zymed), rabbit anti–mouse IgG, and protein A–gold, all at 4°C. Alternatively the cells were fixed with 0.1% glutaraldehyde in 100 mM cacodylate buffer, pH 7.35, washed with glycine-containing buffer, and incubated as above. Prefixation labeling was also performed using a rabbit anti–human placental alkaline phosphatase (Dako) followed directly by protein A–gold.

Labeling with Cholera Toxin-conjugates. A431 cells were washed in DMEM/25mM Hepes (normal medium) or in the above medium with all components at a final concentration of 1.6× (hypertonic medium). Cells were incubated in the same medium containing 0.2% BSA for 1 h before each experiment. The cells were then incubated with CT-B, CT-B–HRP (10 μg/ml), or CT-B–gold, in the same medium at 8°C to optimize labeling of caveolae (Parton, 1994). The cells were then warmed in the appropriate medium in the presence of 1 μM OA for 1 h at 37°C. In some experiments 10 mg/ml horseradish peroxidase (HRP, type II; Sigma) was added during the 37°C incubation.

To distinguish internal from surface caveolae, cells were incubated with CT-B–gold at 4°C, washed, incubated at 37°C under the appropriate conditions and then reincubated at 4°C with 20 μg/ml CT-B–HRP. At this concentration the entire surface was heavily labeled with HRP reaction product. The cells were then embedded in Epon and cut perpendicular to the culture substratum.

Treatment with Cytoskeleton-disrupting Drugs. For disruption of the cytoskeleton, cells were pretreated with cyt D (5 μg/ml) for 15 min or with nocodazole (1.5 μg/ml) for 1 h at 37°C. For immunofluorescence the cells were then incubated with the same drugs plus 1 μM OA for 1 h. For electron microscopy they were incubated with CT-B–HRP at 8°C, washed, and further incubated at 37°C with 1 μM OA all in the presence of either of the two cytoskeleton-disrupting drugs.

Electron Microscopy

Cells were fixed with 2.5% glutaraldehyde in 50 mM cacodylate buffer for Epon embedding or 0.5% glutaraldehyde in 250 mM Hepes for frozen sectioning. They were then processed for frozen sectioning or for Epon sections as previously described (Parton et al., 1992). In some experiments thawed frozen sections were stained after immunogold labeling with a mixture of ammonium molybdate and methylcellulose (Griffiths, 1993).

Cells embedded in a thin layer of Epon were reorientated for sectioning perpendicular to the culture substratum by sandwiching two pieces of Epon together, with the cells innermost and a layer of glue between.

Quantitation of Morphological Experiments. To determine the fraction of the caveolar marker, CT-B–gold, in internal structures (CT-B–HRP negative) versus surface caveolae (CT-B–HRP positive) thin sections were analyzed. Caveolae were recognized by their characteristic size and shape (60-nm diameter, spherical, e.g., see Fig. 3 *C*). Other labeled elements consisted of tubular profiles (e.g., see Fig. 3 *B*) and multivesicular structures (see Fig. 3 *D*). For the sake of the quantitation these structures were grouped together as "endosomes" (Table I). Over 500 gold particles were scored for each condition.

To determine the percentage of the total caveolae which were clustered or isolated, semi-thick sections of CT-B–HRP-labeled cells were cut perpendicular to the substratum. Random fields were photographed at a primary magnification of 12.5kx. Approximately 20 micrographs were examined for each condition. Each caveola, defined as a 60–70-nm spherical profile labeled with CT-B–HRP, was then classified as "clustered" or "isolated" (see Fig. 6).

Immunofluorescence Microscopy

Cells were fixed in methanol at −20°C. Cells were labeled, mounted and viewed as described previously (Chavrier et al., 1990).

Biochemical Measurement of Alkaline Phosphatase Distribution

A431 cells were washed with DMEM/Hepes at 4°C and then reincubated in the same medium with or without sequential incubations with mouse monoclonal antibodies to alkaline phosphatase (Dako) and a rabbit anti–mouse IgG antibody (Cappel, Durham, NC) to induce clustering of alkaline phosphatase (AP) in caveolae. The cells were then warmed to 37°C for various times under different conditions. The alkaline phosphatase distribution was then determined as described by Kobayashi and Robinson (1991). Briefly, cells in multiwell plates were treated as described above, fixed in 1% glutaraldehyde in PBS for 15 min on ice, washed in assay buffer lacking substrate, and then the alkaline phosphatase activity in the presence of 1% Triton X-100 (total AP) or without detergent (surface AP) was determined. In contrast to the surface AP activity, none of the tested reagents consistently changed the total level of AP. However, in some experiments involving long incubations with OA a slight decrease in total AP activity was observed as a result of cell loss.

The times and concentrations for the treatment of cells with various drugs was as described for the morphological experiments. In addition, the following treatments were used; cells were treated for 1 h at 37°C with PMA (2 μM); staurosporine (2 μM) and genistein (4 μM) were both present for 10 min before OA treatment (at 8°C) as well as during the OA treatment. All the above were kept as 1000× stocks in DMSO at −20°C. Incubation of cells with DMSO alone at the same concentration had no effect on the distribution of AP under any experimental condition.

Measurement of Transferrin-HRP Uptake. Incubation of cells with transferrin-HRP (Tf-HRP) (Biotrend, Cologne, Germany) was as described previously for iodinated transferrin (Bucci et al., 1992). In brief, cells were washed, incubated 1 h at 37°C in serum-free medium and then treated for various times at 37°C with 1 μM OA. A 5-min pulse of 25 μg/ml Tf-HRP was added at various times after OA treatment. The cells were then acid-

1. *Abbreviations used in this paper*: AP, alkaline phosphatase; CT-B, cholera toxin-binding subunit; CT-B–gold, CT-B adsorbed to 10 or 14 nm gold; CT-B–HRP, CT-B conjugated to HRP; CytD, cytochalasin D; Tf-HRP, transferrin-HRP; OA, okadaic acid; PMA, phorbol 12-myristate 13-acetate.

Published December 1, 1994

washed, scraped from the culture dish, permeabilized using 0.2% Triton X-100 in 10 mM Hepes for 30 min at room temperature and after centrifugation the HRP activity in the lysate was measured. To check for possible loss of cells during OA treatment the protein concentration in the lysate was assayed by the method of Bradford (1976). All biochemical experiments were performed with triplicates for each condition with the variation shown by the error bars (SE). The results shown are from representative experiments with similar results in at least three separate experiments.

Results

Antibody-induced Clustering of Alkaline Phosphatase in Caveolae of A431 Cells

Alkaline phosphatase is a well-characterized GPI-anchored protein which has been shown to be present within caveolae after cell surface labeling (Ying et al., 1992). Conditions were optimized for antibody-induced clustering of AP in caveolae of A431 cells using electron microscopy. Cells labeled at 4°C with primary antibody followed by a second antibody and protein A–gold showed clusters of gold particles within caveolae (Fig. 1 *A*). Little labeling was found over the remainder of the plasma membrane. Quantitation showed that 61 ± 12% of the labeling was found in caveolae under these conditions. Less than 0.3% of the labeling was found within clathrin coated pits. Similar results were obtained using a rabbit anti-AP antibody followed directly by protein A–gold with 56% of the surface gold within caveolae. In contrast, cells labeled after fixation showed labeling over the entire surface with no preferential labeling of caveolae (Fig. 1 *B*) consistent with results with other GPI-anchored proteins (Mayor et al., 1994).

Alkaline Phosphatase Activity as a Marker of Surface vs Intracellular Caveolae

AP activity can be assayed using p-nitrophenyl phosphate as substrate at pH 9.5. Total and surface AP are determined in the presence or absence of detergent, respectively (Kobayashi and Robinson, 1991), the difference between the two representing the intracellular pool of AP. As the substrate is a small molecule its accessibility to the AP is a good indication of whether the enzyme is actually on the surface or within the cell. This is an important consideration as groups of caveolae may be attached to the plasma membrane by long thin tubules (see Fig. 3). We first optimized the conditions for AP detection in A431 cells. Surface AP was shown to represent 74 ± 9% (mean of eight separate experiments) of the total cellular AP. Some variation in the level of surface AP was found between experiments but within each experiment variation within the triplicate was ~5%. Antibody addition, to induce crosslinking and clustering of AP in caveolae, did not change the total AP activity.

We examined whether incubating cells at 37°C, with or without antibody addition, caused a shift in the distribution of AP activity. In the absence of antibodies no change in the relative level of surface AP activity occurred (Fig. 2 *A*). However, after crosslinking a small but significant decrease

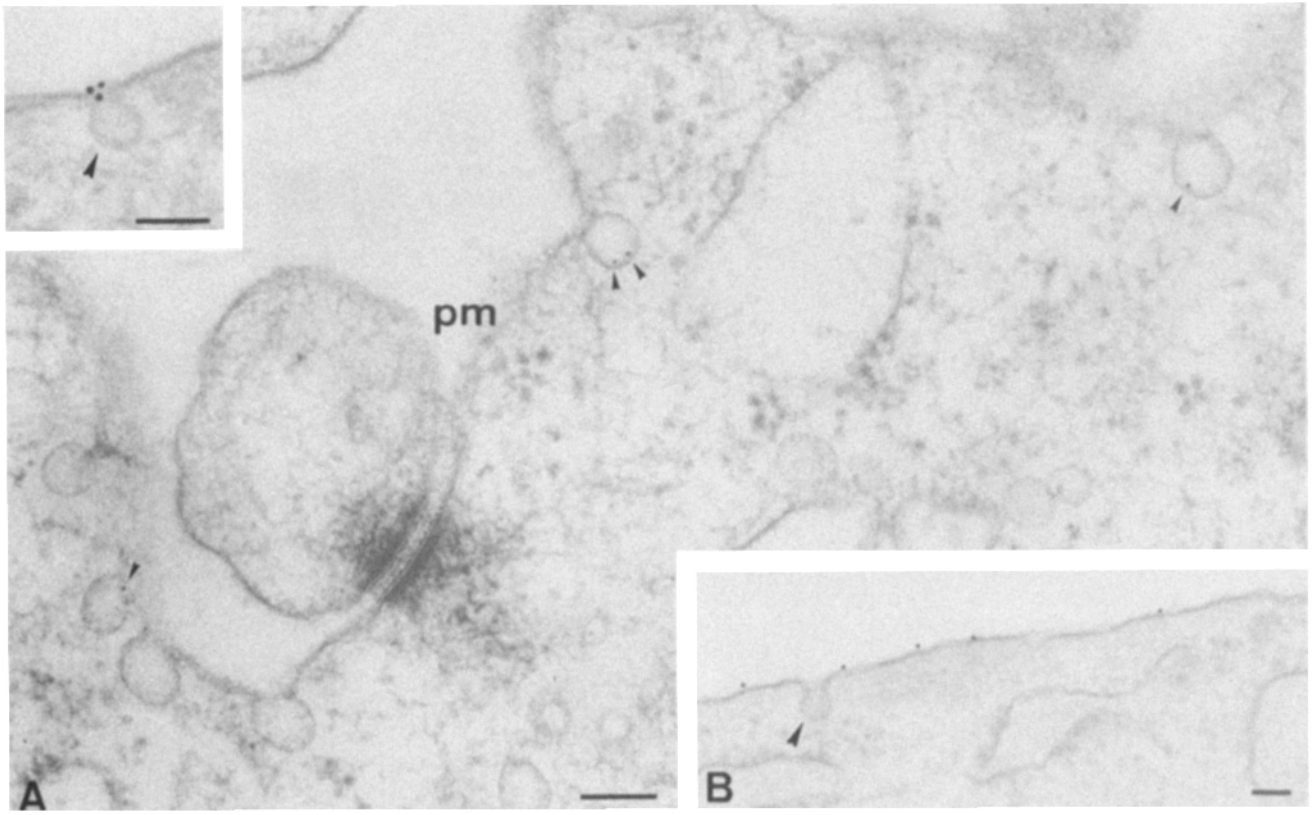

Figure 1. Surface labeling of alkaline phosphatase in A431 cells. Cells were incubated with antibodies to AP followed by second antibodies and 5 or 10 nm protein A-gold either before (*A*) or after (*B*) glutaraldehyde fixation. Cells labeled at 4°C before fixation show labeling within caveolae at the cell surface (*arrowheads*). In contrast, cells labeled after a mild glutaraldehyde fixation show labeling over the entire surface with little concentration within caveolae (*arrowhead*). pm, plasma membrane. Bars, 100 nm.

Published December 1, 1994

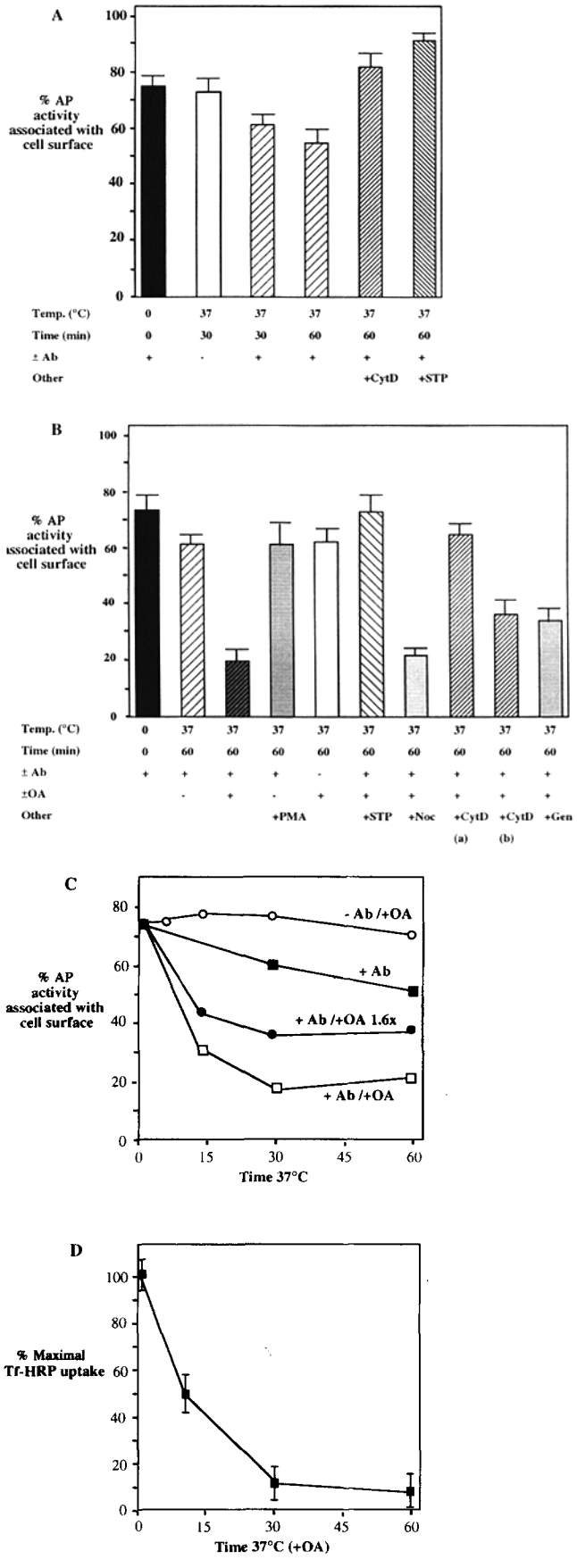

in surface AP activity occurred which was significant after 30 min at 37°C. We assume that this difference is due to the clustering of the alkaline phosphatase within caveolae after antibody binding. No change in the relative distribution of AP was observed if the cells were kept at 4°C after antibody addition. We also tested whether the redistribution of AP was dependent on cytoskeletal elements. While nocodazole had no effect, CytD blocked the decrease in surface AP which occurred on warming the cells and caused a small but consistent increase in surface AP (Fig. 2 *A*).

Okadaic Acid Stimulates, and Staurosporine Inhibits, the Internalization of Cross-linked AP

We tested a number of agents which may affect the function of caveolae. First, we examined the effect of hyperphosphorylation on AP distribution by using the general phosphatase inhibitor okadaic acid (OA, Cohen et al., 1990). OA caused a striking decrease in surface AP (Fig. 2 *B*). The maximal effect was seen after around 30 min at 37°C when only 20% of the AP activity remained on the surface (Fig. 2 *C*). To determine the specificity of the OA effect, we treated cells with OA in the absence of antibody binding when the AP labeling should be distributed over the entire surface and not concentrated in caveolae (Fig. 1). No significant decrease in surface AP was observed at any time (Fig. 2, *B* and *C*). This shows that the effect of OA was not due to a general stimulation of plasma membrane internalization and is consistent with the low density of GPI-anchored proteins detected in caveolae in the absence of an antibody cross-linking step (see above, and Mayor et al., 1994). Consistent with the expected role of kinases in the OA effect, staurosporine, a general kinase inhibitor, completely blocked the effects of OA (Fig. 2 *B*). Interestingly, staurosporine also blocked the decrease in surface AP activity observed in the absence of OA and even caused a small but consistent increase in surface AP activity (Fig. 2 *A*). Staurosporine treatment did not affect the clustering of AP in caveolae (results not shown). These results strongly suggest that the internalization of clustered AP is dependent on the relative activity of kinases and phosphatases. Genistein, which shows higher specificity for tyrosine kinases, had only a partial effect on the OA-induced redistribution (Fig. 2 *B*). We also examined

Figure 2. Biochemical detection of surface and intracellular alkaline phosphatase A-C. A431 cells were treated with or without antibodies to AP followed by a second antibody. They were then fixed immediately or treated with the agents indicated (as described in Materials and Methods) before fixation. CytD was used at two different concentrations, (*a*) 10 μg/ml and (*b*) 1 μg/ml. Surface and total AP were assayed and the results were expressed in terms of the percentage of total AP which is on the cell surface. Results are expressed as the mean with the standard error indicated (*A*, *B*, and *D*). *C* shows time courses for the redistribution of surface AP after treatment with OA without an antibody-incubation step (*-Ab/+OA*), after antibody binding only (*+Ab*), and after antibody binding and OA treatment in hypertonic (*+Ab/+OA 1.6x*) or normal (*+Ab/+OA*) medium. (*D*) Cells were treated with OA for various times and then incubated with a 5-min pulse of Tf-HRP. After removing surface Tf-HRP the cell-associated HRP activity was determined and expressed as the fraction of the maximal Tf-HRP uptake (in the absence of OA). *gen*, genistein; *Noc*, nocodazole; *STP*, staurosporine.

Published December 1, 1994

the effect of the protein kinase C activator, PMA, on the AP distribution. PMA has previously been shown to prevent potocytosis and decrease the number of surface caveolae (Smart et al., 1993). Consistent with previous results with A431 cells (Sandvig and van Deurs, 1990), PMA increased fluid-phase marker uptake (results not shown) but after a 1-h incubation there was no significant change in the level of surface AP (Fig. 2 *B*). Next we examined the effect of cytoskeleton-disrupting agents on the OA-induced redistribution of AP. While nocodazole had no effect, CytD blocked the OA effect in a concentration-dependent manner; in the presence of 1 μg/ml CytD okadaic acid caused only a 50% decrease in surface AP activity whereas 10 μg/ml CytD completely blocked the effects of OA (Fig. 2 *B*).

Finally, we investigated the effect of OA on the clathrin-coated pit uptake pathway. A 5-min pulse of Tf-HRP was administered at various times after OA treatment. The cell-associated HRP activity was then measured after removal of the surface Tf-HRP. As shown in Fig. 2 *D* the coated pit pathway is rapidly inhibited under these conditions. After 5 min the activity is already reduced by 50% and after 15 min by 80% consistent with previous studies of the effects of OA on the endocytic pathway (Lucocq et al., 1991; Lucocq, 1992). This argues against any involvement of the coated pit internalization pathway in the redistribution of AP under these conditions.

Electron Microscopic Analysis of the Effects of OA on Caveolae

We employed electron microscopy to further investigate the caveolae dynamics. As an independent marker, we used cholera toxin-binding subunit adsorbed to gold (CT-B–gold), a single step labeling reagent which is highly specific for caveolae (Parton, 1994). After washing, the cells were kept at 4°C or warmed for various times to 37°C. After this incubation the cell surface was labeled at 4°C with cholera toxin-binding subunit conjugated to HRP (CT-B–HRP). CT-B–HRP labels the entire cell surface but is concentrated within caveolae (see e.g., Figs. 3 *A* and 6 *A*). This allowed us to ascertain whether gold-labeled structures were still attached to the surface (CT-B–gold and CT-B–HRP positive) or were now internal (CT-B–gold positive, CT-B–HRP negative).

In cells treated with CT-B–gold and then labeled with CT-B–HRP without a warming step, all the gold was accessible to the second marker despite the double labeled structures occasionally appearing deep within the cell (Fig. 3 *A*). 62% of the gold was found within caveolae (Table I) and only 1.8% within clathrin coated pits. After a warming step a small fraction of the cholera toxin-gold became internalized and gold particles were observed in CT-B–HRP-negative tubules, endosomes and caveolae-like structures (Fig. 3, *B–D*). We then examined the effect of OA on the surface caveolae. Labeling of internal caveolae-like profiles, multivesicular endosomes, and putative endosomal tubules were all increased upon OA treatment (Fig. 3 *E*, Table I). Consistent with the decrease in gold within surface caveolae, the mean number of surface caveolar profiles per cell was decreased ninefold after a 15-min incubation in the presence of OA. Serial section analysis (results not shown) and thick section electron microscopy after CT-B–HRP and HRP internalization suggested that the majority of the caveolae, if not all, were present in large clusters or attached to tubular elements rather than being present as free-budded caveolae (see e.g., Fig. 3 *F*). Quantitation showed that the fraction of internal gold increased from 35% after a 15-min incubation in the absence of OA to 86% after incubation for the same time but in the presence of 1 μM OA (Table I). The fraction of gold within internal caveolar profiles and putative endosomal elements were both increased upon OA treatment (Table I; see Materials and Methods for details). As OA treatment inhibits the clathrin coated pit pathway, this suggests that caveolar domains can fuse with endosomes. Examination of the pattern of CT-B–HRP or HRP labeling in semi-thick sections after OA treatment for 15-min showed labeling of a heterogeneous population of tubulovesicular elements including multivesicular endosomes and caveolar-like profiles (see e.g., Fig. 3 *F*). Consistent with the biochemical results, CytD blocked the OA-induced internalization of CT-B–gold without affecting the caveolar morphology or the clustering of the gold within caveolae (results not shown, also see Fig. 9 *I*).

Okadaic Acid Treatment in Hypertonic Medium Causes Redistribution of VIP21/Caveolin

We investigated whether OA has any effect on the distribution of VIP21/caveolin using a specific antibody against the NH_2-terminus of the protein (here referred to as VIP21N/caveolin) which only recognizes the caveolar form of the protein (Dupree et al., 1993). Immunofluorescence experiments showed that VIP21N/caveolin labeling generally appeared more diffuse after OA treatment but in some cells patches of intracellular labeling were apparent (Figs. 4 *B* and 9 *C*). We attempted to optimise this effect and fortuitously found that treatment of cells with OA in the presence of hypertonic (1.6× concentrated) medium exaggerated this effect of OA. OA treatment under these conditions caused a dramatic effect on VIP21N/caveolin distribution; in all cells the labeling redistributed from the cell surface to intracellular patches between 30 and 60 min at 37°C (Figs. 4 *C* and 9 *E*). The hypertonic medium alone had no effect on cell morphology or viability even after 24 h. The effect of OA in the hypertonic medium, as determined biochemically by the effect on surface AP, was similar to, but less dramatic, than the effect of OA in the normal medium (Fig. 2 *C*). The redistribution of VIP21/caveolin under these conditions as judged by immunofluorescence was also blocked by staurosporine (results not shown). We then used immunoelectron microscopy to find out where the VIP21/caveolin was localized within the cell. After treatment of the cells with OA for 1 h at 37°C, heavy labeling for VIP21N/caveolin was apparent on large clusters of vesicular profiles close to the nucleus (Fig. 5) and occasionally the centrioles (e.g., Fig. 5 *A*). The labeled structures often resembled the interconnected groups of caveolae seen occasionally in control cells (Fig. 5 *D*, compare with e.g., Fig. 3 *A*). This suggested that these structures are clusters of caveolae which have redistributed from the periphery of the cell. This was confirmed using CT-B–HRP which was bound to the cell surface at 8°C before OA treatment. After treatment of cells with OA for 1 h at 37°C, semi-thick section electron microscopy demonstrated the presence of extremely large clusters of caveolae (Fig. 6) close to the nucleus and usually near to the dorsal pole of the cell (Fig. 6 *B*). In the absence of OA, CT-B–HRP showed only weak

Published December 1, 1994

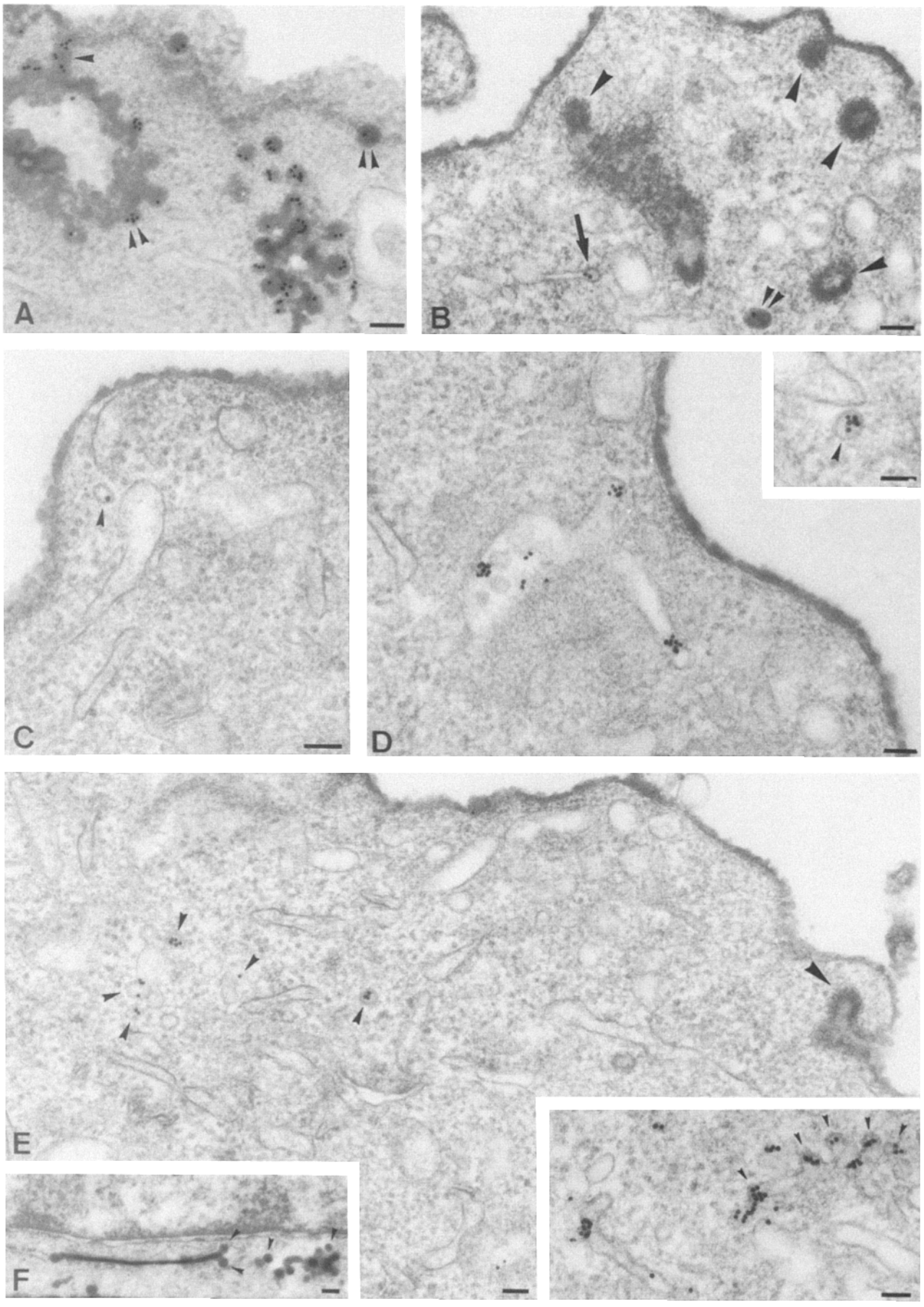

Published December 1, 1994

Table I. Quantitative Analysis of CT-B-Gold Distribution After OA Treatment

Condition 37°C	% gold on surface	% gold within cell	% gold in surface caveolae	% gold in internal caveolar profiles	% gold in endosomal profiles*
0	100	0	62	0	0
15 min	65	35	49	7	28
60 min	47	53	39	6	50
15 min + OA	14	86	7	43	43

* Includes internal tubular profiles and multivesicular endosomes. See Materials and Methods for details.

labeling of Golgi elements and occasionally endosomes (results not shown). The percentage of caveolae present as clusters rather than single caveolae dramatically increased from 22 (under control conditions) to 80% (after treatment with OA for 1 h). Rarely were caveolae found at the periphery of the cell. Tubular profiles, apparently derived from the plasma membrane, occasionally appeared to be connected to the clusters of vesicles (Fig. 6 *B*). The labeled structures were shown to be VIP21/caveolin positive (Fig. 7 *B*) and distinct from the typical Golgi clusters described previously (Fig. 7 *C*; Lucocq et al., 1989, 1991). CT-B-gold particles were observed in the 60-nm buds and not in the associated tubules (Fig. 7 *A*). HRP included in the medium as a fluid-phase marker during the OA treatment labeled the CT-B-gold-positive structures and the associated tubules (Fig. 7, *A* and *C*). As the cells were washed for 1 h at 4°C before fixation the results suggest that most of the gold-labeled HRP-containing structures were no longer connected to the plasma membrane (Fig. 7, *A* and *C*) consistent with the biochemical results. In contrast to the cells treated with OA in normal medium, the caveolar clusters formed in the hypertonic medium were the major structures labeled with HRP. Transferrin-HRP bound to the cell surface before, or during, OA treatment did not appear in CT-B-gold labeled caveolae after a 1-h treatment with OA (results not shown).

The effect of OA in the hypertonic medium was reversible. At an intermediate time after washing out the OA (3 h) some cells had already flattened and both surface and intracellular labeling for VIP21/caveolin was apparent (Fig. 4 *C*). The intracellular labeling was present in large patches within the cytosol. At this time large clusters of CT-B-HRP labeled caveolae were evident in the perinuclear area of the cell (Fig. 8). These clusters could also be labeled by adding a pulse of HRP at the time of OA treatment and then incubating the cells a further 3 h in the absence of OA and HRP (Fig. 8 *C*). Later the intracellular clusters disappeared and VIP21/caveolin labeling was only found at the cell surface (results not shown).

Interaction of Caveolar Clusters with the Cytoskeleton

Since the internalization of caveolar AP was completely blocked by treatment of the cells with CytD, we examined whether the OA-induced redistribution of caveolar clusters to the center of the cell in hypertonic medium was also affected by CytD. Cells were treated for 15 min with 5 μg/ml CytD and subsequently treated with OA, also in the presence of CytD. For this analysis we used MDCK cells grown on coverslips which remained flat during OA-treatment, facilitating light microscopic analysis. As in A431 cells, VIP21/caveolin labeling was redistributed from the lateral border of the cell to the perinuclear area after OA treatment in hypertonic medium whereas in normal medium the labeling became more diffuse (Fig. 9, *A–F*). The change in distribution upon OA treatment in hypertonic medium was completely blocked by treatment of CytD (Fig. 9, *G–I*) as confirmed by electron microscopy of A431 cells (Fig. 9 *I*). Under these conditions only 24% of the caveolae were present as clustered structures as in untreated cells.

Although nocodazole had no effect on the internalization of caveolae, we examined whether the movement of the caveolar clusters to the cell center was affected by microtubule depolymerization. By indirect immunofluorescence, VIP21N/caveolin labeling was shown to be concentrated around the microtubule-organizing center of many OA-treated MDCK cells (Fig. 10). MDCK cells in hypertonic medium were treated with nocodazole and then with OA, again in the presence of nocodazole. Under these condi-

Figure 3. Effect of OA on surface caveolae. *A–E* show examples of the morphological assay used to assess surface connectivity of CT-B-gold-labeled structures. Cells were incubated with CT-B-gold at 4°C and then incubated for various times at 37°C in the presence (*E* and *F*) or absence of OA (*B–D*). The cells were then returned to 4°C and incubated with CT-B-HRP to label the cell surface. (*A*) Cells were incubated with CT-B-gold followed by CT-B-HRP without a warming step between. This semi-thick section (~200 nm) shows a group of caveolae which are attached to the cell surface (an arrowhead marks a connecting structure). All the gold is within CT-B-HRP positive caveolae evident as 60–70-nm invaginations (*double arrowheads*). (*B–D*) Cells were surface-labeled with CT-B-gold and then incubated for 15 min at 37°C before labeling the cell surface at 4°C. (*B*) Note the CT-B-HRP-labeled clathrin-coated pits (*arrowheads*) which must be connected to the cell surface out of the plane of section. The double arrowheads mark a surface-connected caveola containing both CT-B-HRP and CT-B-gold. Two gold particles are evident within an internal tubular/cisternal structure (*arrow*) which is CT-B-HRP negative. *C* and *D* show examples of internal structures labeled with CT-B-gold only. *C* and the inset show examples of possible caveolae while in *D* two gold-containing tubular profiles are connected to a multivesicular endosome. (*E*) Cells were labeled as above but were incubated for 15 min in the presence of OA. Gold particles are evident within CT-B-HRP negative vesicular and tubular profiles as shown at higher magnification in the inset. Note the 60–70 nm buds/vesicular profiles (*small arrowheads*). A surface clathrin-coated pit is indicated (*large arrowhead*). *F* shows a semi-thick section of a cell incubated as above but with CT-B-HRP surface labeling before OA treatment. Note the clusters of caveolae-like structures (*arrowheads*) which are often associated with tubular elements. Bars: (*A–E*) 100 nm, (*F*) 200 nm.

Published December 1, 1994

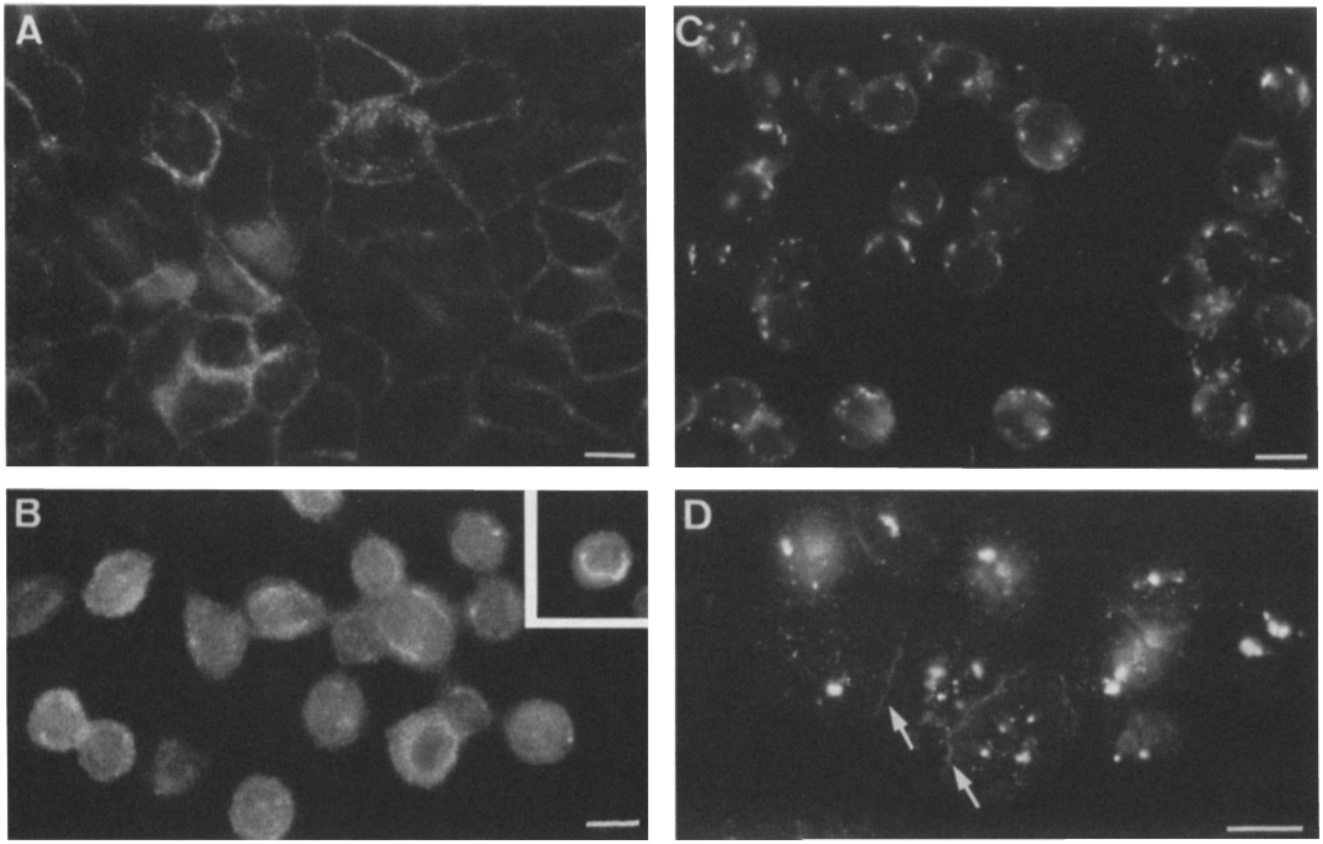

Figure 4. Localization of VIP21N/caveolin in okadaic acid-treated A431 cells. A431 cells were treated with 1 μM okadaic acid for 1 h in normal medium (*B*), or in hypertonic medium (*C*). *A* shows control cells. *D* shows cells treated as in *C* and then incubated in OA-free hypertonic medium for 3 h before fixation. All cells were then labeled for VIP21N/caveolin. Untreated cells (*A*) show characteristic lateral staining of the plasma membrane. After treatment with OA (*B*), the cells round up and diffuse labeling is evident. Some cells show patches of labeling (see inset). In contrast, after OA treatment in hypertonic medium, essentially all the labeling is concentrated in discrete areas close to the nucleus. After removal of OA (*D*) and reincubation in OA-free hypertonic medium the cells flatten. Some VIP21N/caveolin is evident at the cell periphery (*arrows*), but in most cells patches of perinuclear staining are still apparent. Bars, 10 μm.

tions all microtubules were depolymerized as judged by indirect immunofluorescence using an anti-tubulin antibody (results not shown). VIP21/caveolin was found to be distributed throughout the nocodazole/OA-treated cells in relatively large structures, often peripherally, and was not concentrated in the perinuclear area (Fig. 9, *J* and *K*). These results were confirmed by electron microscopy using A431 cells (Fig. 9 *L*). Quantitation demonstrated that under these conditions 69% of the caveolae were clustered, similar to cells treated in the hypertonic medium with OA alone.

Discussion

In the present study we have shown that okadaic acid, a specific inhibitor of phosphatases 1 and 2a, caused a dramatic removal of caveolae from the cell surface. To examine this process further we developed a biochemical assay for caveolar internalization. Using this assay we have been able to show that the OA-induced removal of a GPI-anchored protein from the cell surface was blocked by a general kinase inhibitor and by CytD, and was dependent on the clustering

Figure 5. Immunoelectron microscopic localization of VIP21N/caveolin in A431 cells treated with OA in hypertonic medium. A431 cells were treated with OA for 1 h in hypertonic medium and then fixed and processed for frozen sectioning. Sections were indicated by anti-VIP21N/caveolin antibodies followed by protein A-gold. Heavy labeling of tubulovesicular elements close to the nucleus (*n*) and centrioles (*c*) is apparent (*A*). A common observation is the presence of intermediate filaments (*i*) close to the labeled elements (also see Figs. 4, *B* and *C* and 5 *C*). The labeled structures are shown at higher magnification in *B–D*. Note that the labeling is associated with the 60-nm buds (*arrows*) and not the associated tubules (*C*, *arrowheads*). *D* shows a labeled section which was stained with ammonium molybdate to more clearly delineate the structure of the labeled elements. The labeled structures resemble caveolar rosettes (also see structure indicated by arrows in *A*). Bars, 100 nm.

Published December 1, 1994

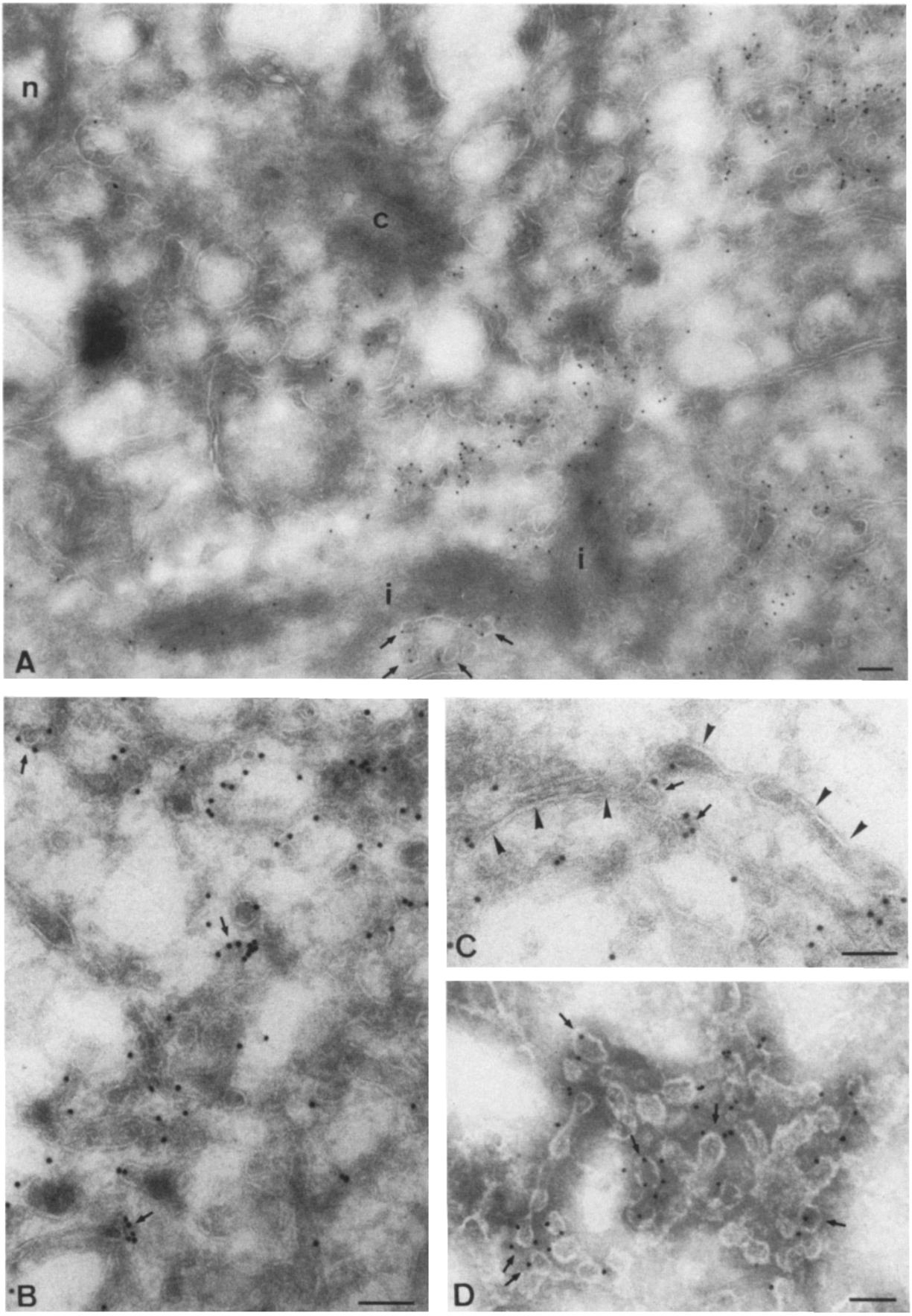

Published December 1, 1994

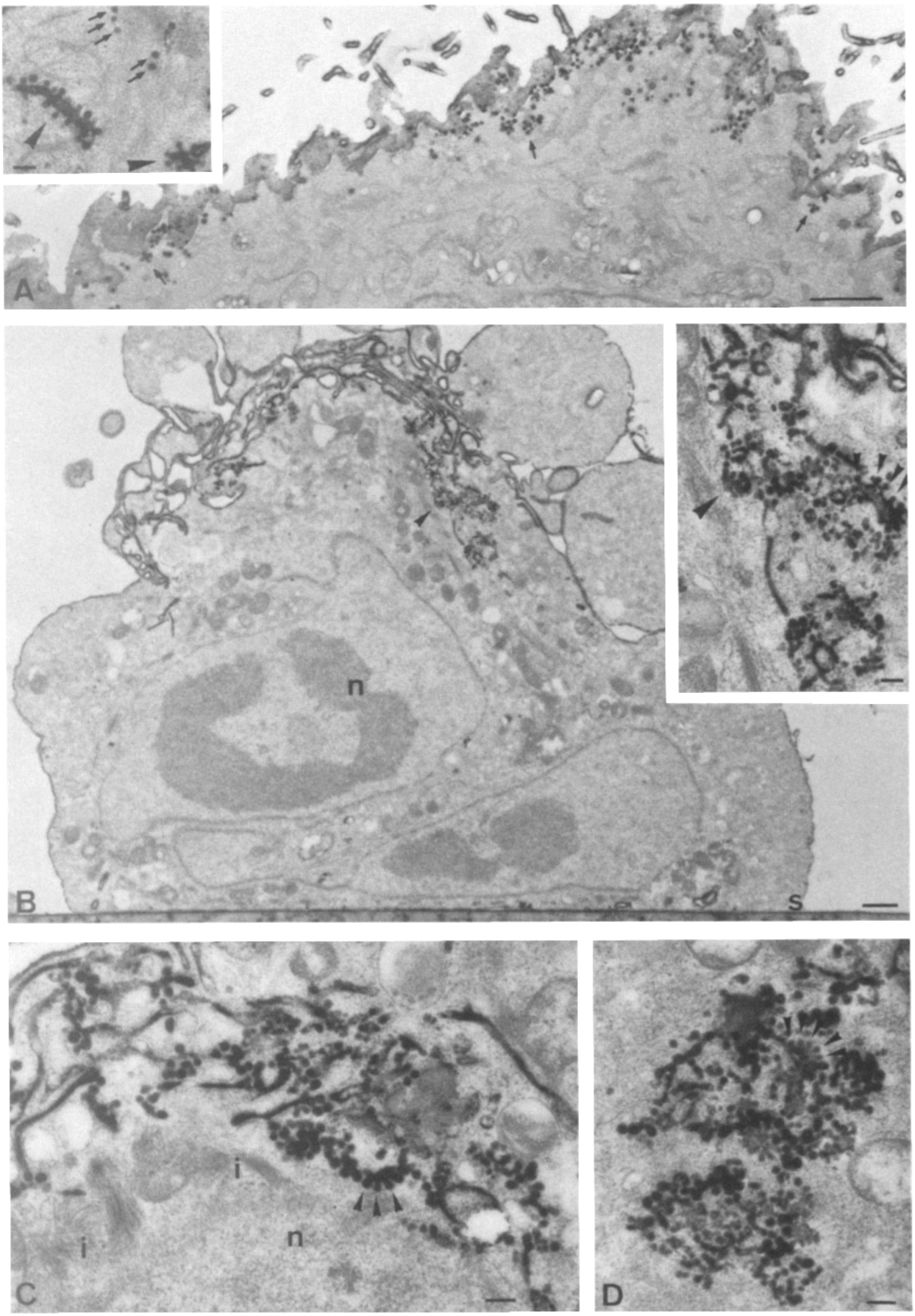

Figure 6. Distribution and morphology of CT-B–labeled structures in control and OA-treated A431 cells. A431 cells were labeled with CT-B–HRP and then fixed (*A*) or warmed in the presence of OA in hypertonic medium (*B–D*). After Epon embedding semi-thick (200 nm) sections were prepared. *A* shows a low magnification view of a cell which was surface-labeled with CT-B–HRP at 8°C. Caveolae

Published December 1, 1994

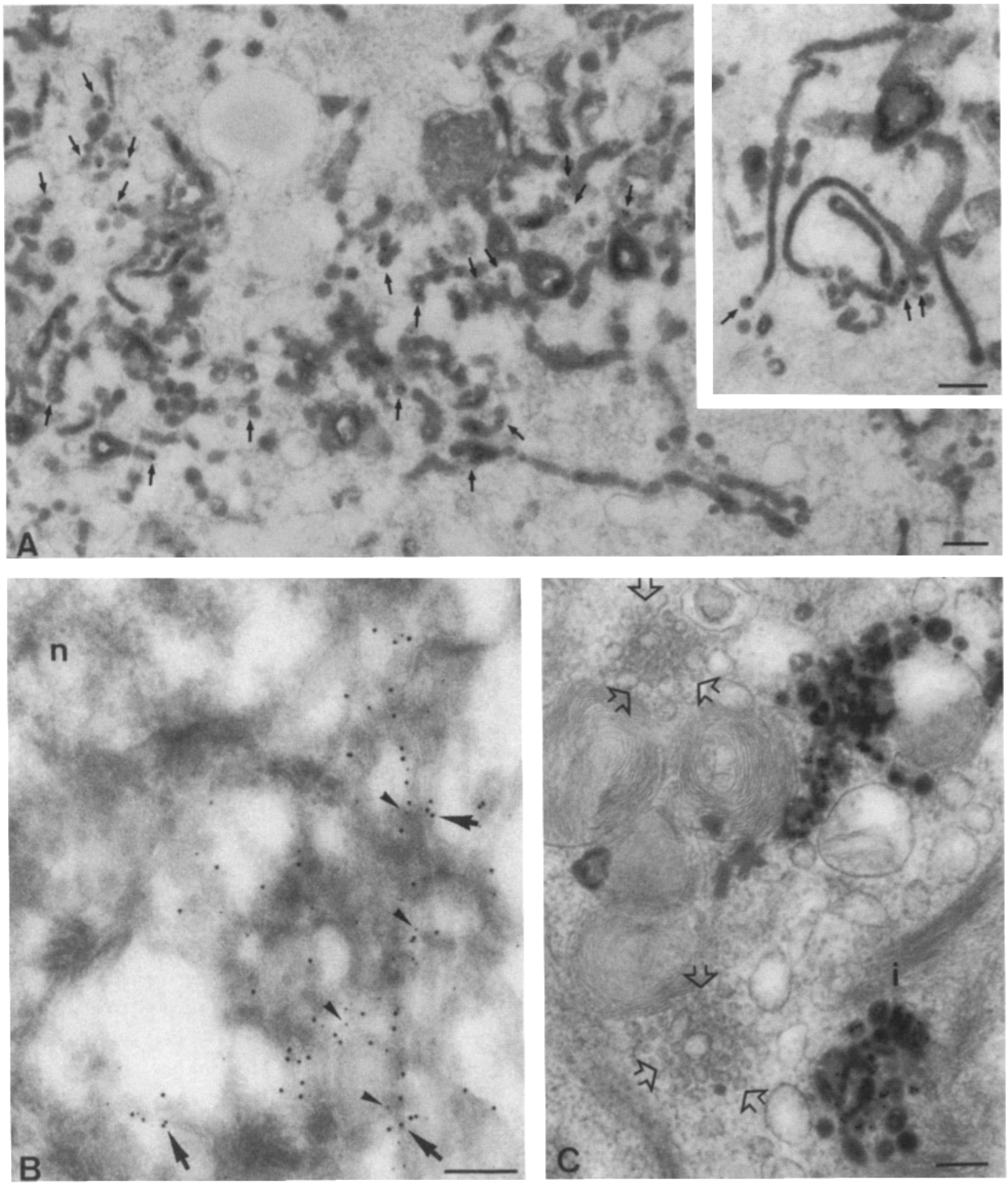

Figure 7. Morphology of CT-B–labeled structures in OA-treated A431 cells. 431 cells were labeled with CT-B–gold (*A* and *C*) or unlabeled CT-B (*B*) at 8°C and then washed and warmed in the presence of OA as described in the legend to Fig. 4. *A* and *C* show semi-thick Epon sections. The cells were surface-labeled with CT-B–gold and then warmed in the presence of OA and HRP for 1 h. Numerous tubular structures containing HRP are evident but only the buds at the ends of the tubules contain CT-B–gold (*arrows*). *B* shows the perinuclear area of a cell which was labeled with CT-B and then warmed in the presence of OA for 1 h before processing for frozen sections. Ultrathin sections were then labeled with antibodies to VIP21N/caveolin followed by 10 nm gold (*large arrows*) and anti-cholera toxin followed by 6 nm gold (*small arrowheads*). The two markers colocalize in structures close to the nucleus (*n*). *C* shows a cell labeled with CT-B–gold and HRP as described above. Two discrete clusters of small vesicles (indicated by *open arrowheads*) with the characteristics of Golgi clusters are not labeled by the HRP or CT-B–gold. *n*, nucleus. Bars, 200 nm.

(*arrows*) are distributed over the entire cell surface. The inset shows a characteristic cluster of caveolae (*arrowheads*) in comparison to single caveolae (*arrows*). (*B*) After OA treatment CT-B–HRP-labeled structures are observed in groups (one group indicated by an arrowhead is shown at higher magnification in the inset) at the dorsal pole of the cell. Note that few caveolae are seen on the remainder of the plasma membrane. Each group comprises tubules with attached buds of 50–70-nm diameter as shown at higher magnification in the inset and in *C* and *D*. Note the rosette-like structures (*arrowheads* indicate some of the buds). *n*, nucleus; *i*, intermediate filaments; *s*, culture substratum. Bars; (*A* and *B*) 1 μm; (*C* and *D*, insets) 200 nm.

Published December 1, 1994

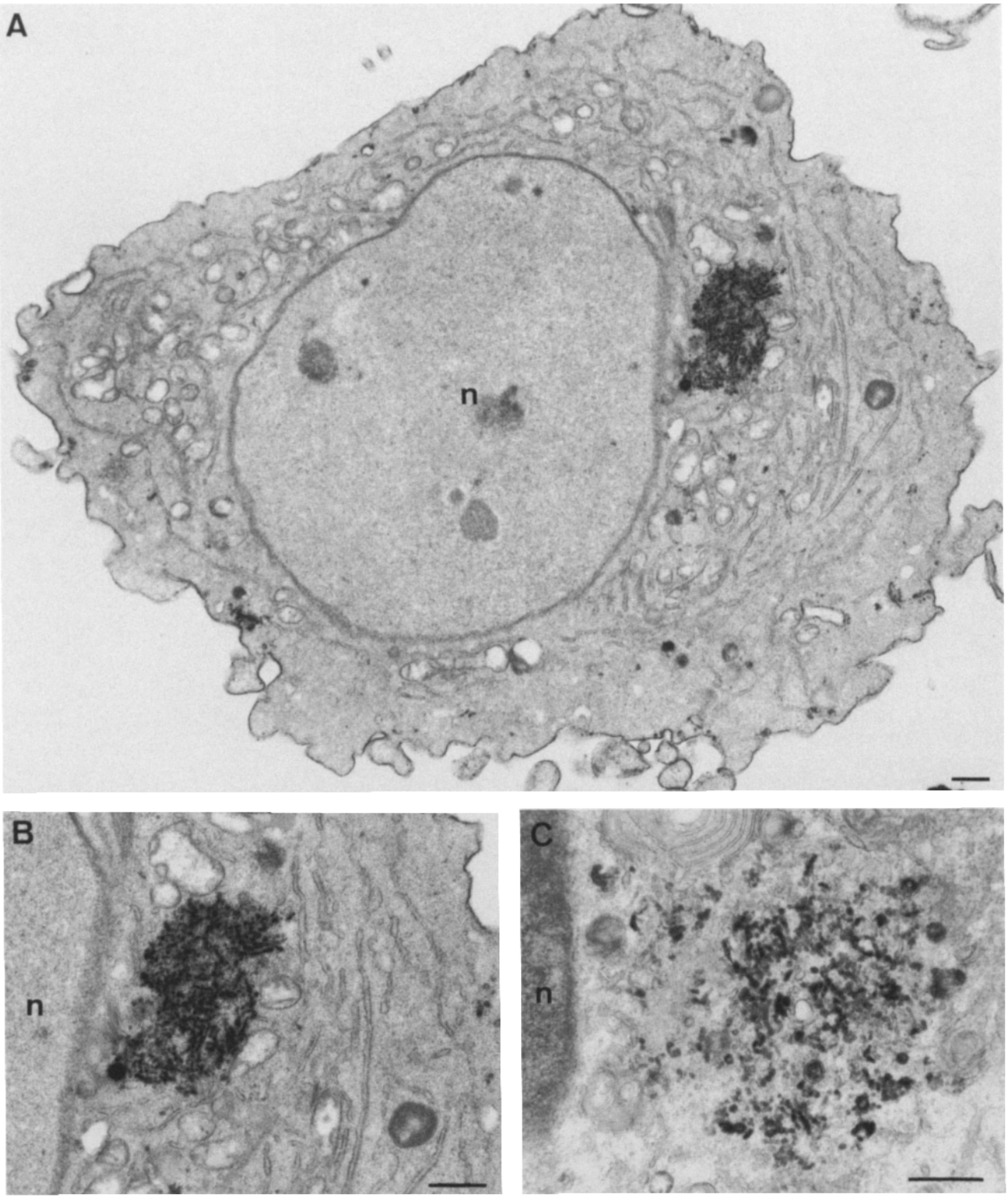

Figure 8. Morphology of caveolae after OA wash-out. (*A* and *B*) A431 cells were labeled with CT-B–HRP and then washed and warmed in the presence of OA as described in the legend to Fig. 4. The cells were then washed and reincubated for a further 3 h in the absence of OA, also in hypertonic medium. After Epon embedding semi-thick (200 nm) sections were prepared. *A* shows a low magnification view of a typical cell. A cluster of CT-B–HRP-labeled structures is located close to the nucleus (*n*). As shown at higher magnification in *B* the labeled structure has the morphology of a caveolar cluster. (*C*) A431 cells were incubated with HRP and OA for 1 h and then washed and reincubated in HRP- and OA-free medium. A caveolar cluster close to the nucleus is labeled with HRP. Bars, 1 μm.

Published December 1, 1994

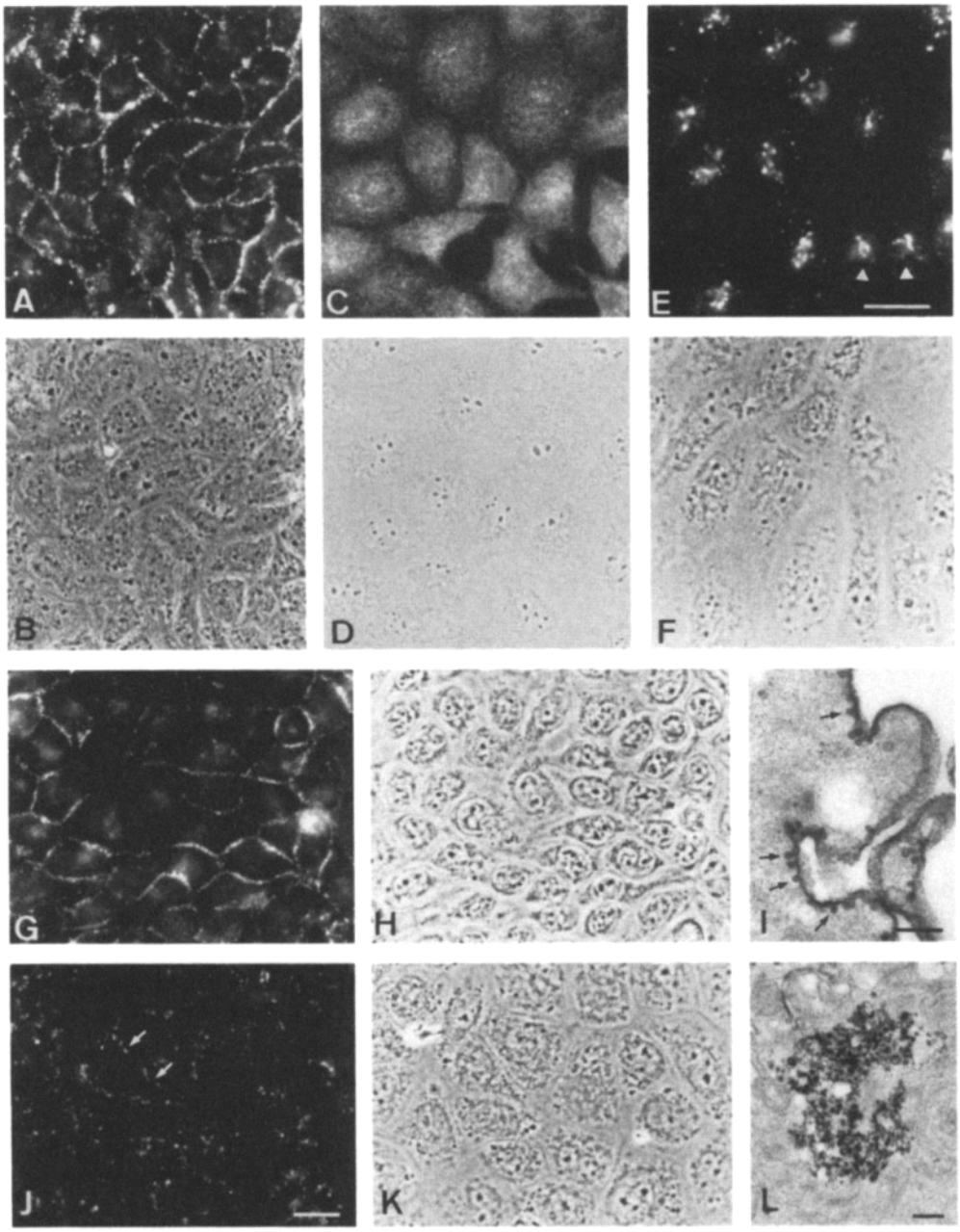

Figure 9. Effect of cytoskeleton disrupting agents on the OA-induced redistribution of caveolae. MDCK cells were treated with OA only (*C–F*), with OA and CytD (*G* and *H*, or with OA and nocodazole (*J* and *K*). All incubations with OA were for 1 h and were either in normal medium (*C* and *D*) or in hypertonic medium (*E–L*), as described in Materials and Methods. The cells were then fixed and VIP21N/caveolin was detected by indirect immunofluorescence (*A*, *C*, *E*, *G*, and *J*). *B*, *D*, *F*, *H*, and *K* show the corresponding phase contrast images. Control cells (*A* and *B*) show the characteristic staining of the lateral plasma membrane area. After OA treatment in normal medium, labeling is evident in small dots (*C* and *D*). In contrast, after OA treatment in hypertonic medium (*E* and *F*) labeling is observed in large patches in the perinuclear area of each cell (*small triangles* in *E* indicate two nuclei). Note that the cells do not round up significantly under these conditions. Cells treated with both CytD and OA in hypertonic medium show no redistribution of VIP-labeling (*G* and *H*). In cells treated with nocodazole and OA (*J* and *K*), labeling is not clustered in the perinuclear area as in cells treated with OA alone (compare with *C* and *E*). Labeling is present in the cell periphery, in some cases lying close to the lateral plasma membrane (*arrows*), but the labeling pattern is clearly different from control untreated cells (compare with *A*). *I* and *L* show regions in the periphery of A431 cells which were labeled with CT-B–HRP and then treated with OA and CytD (*I*) or OA and nocodazole (*L*). Note that CytD completely blocks the redistribution of caveolae which remain at the cell periphery (*I*, *arrows*), whereas clusters still form in the presence of nocodazole (*L*). Bars; (*A–H*, *J* and *K*) 10 μm; (*I* and *L*) 0.5 μm.

of the GPI-anchored protein into caveolae prior to OA treatment. Filipin, which disrupts the structure of caveolae and prevents clustering of GPI-anchored proteins (Rothberg et al., 1990*a*, 1992; Chang et al., 1992), also blocked the decrease in surface AP in the presence or absence of OA, without significantly affecting transferrin uptake (Parton R. G., and B. Joggerst, results not shown). These results, as well as the decrease in internalization via clathrin coated pits after OA treatment, strongly suggest that the effect of OA is specific for caveolae rather than generally causing plasma membrane internalization. In the absence of OA a caveolar marker was also internalized, although at a slower rate, and this process was also blocked by a kinase inhibitor. This suggests that OA may simply be exaggerating a normally occurring but low frequency process and that the internalization of caveolae may be regulated by phosphorylation and dephosphorylation. OA treatment in hypertonic medium allowed the visualization of a possible intermediate in the redistribution process when clusters of caveolae accumulated in the center of the cell.

Previous work has described an internalization pathway for toxin-gold conjugates via small uncoated invaginations

Published December 1, 1994

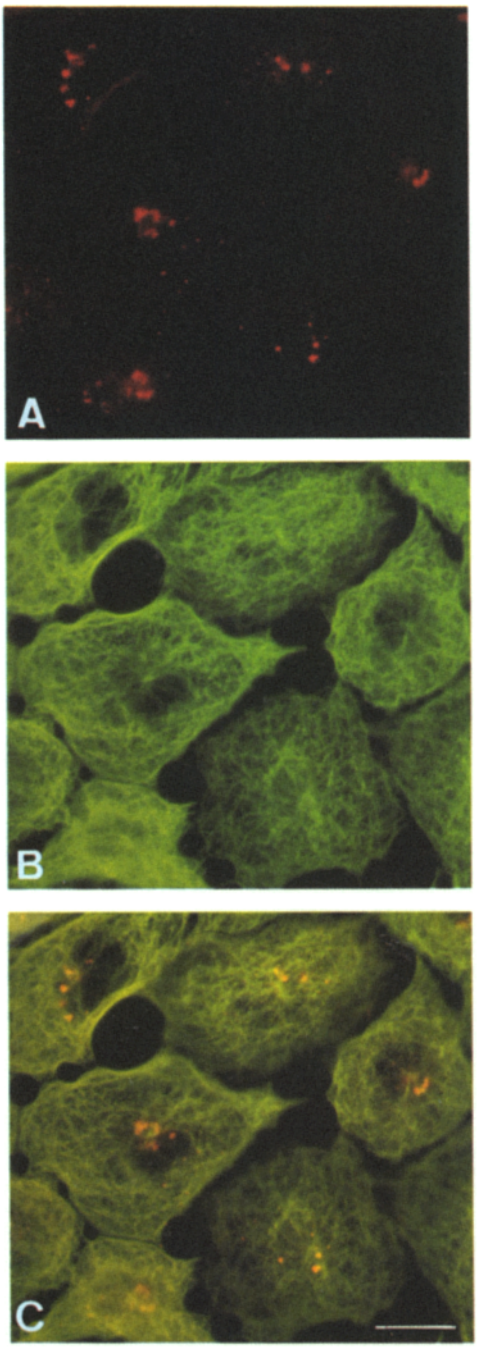

Figure 10. Microtubule organization in OA-treated MDCK cells. A431 cells were treated with OA in hypertonic medium for 1 h at 37°C, fixed and then VIP21N/caveolin and tubulin were detected by indirect immunofluorescence. *A* shows the distribution of VIP-21N/caveolin and *B* shows the microtubule organization. The double exposure (*C*) shows that the VIP21N/caveolin staining (*red*) colocalizes with the microtubule-organizing centers (microtubules in green). Bar, 10 μm.

(Montesano et al., 1982; Tran et al., 1987; Parton et al., 1988; Carpentier et al., 1989). These structures were subsequently shown to be caveolae as defined by VIP21N/caveolin labelling (Parton, 1994). Morphological studies by Orci and coworkers delineated the internalization pathway which involved the budding of caveolae to generate non-coated vesicles and their fusion with tubulovesicular elements in the cell periphery (Montesano et al., 1982; Tran et al., 1987). GPI-anchored proteins have also been shown to internalize into endosomes (Hjelle et al., 1991; Birn et al., 1993; Turek et al., 1993). For example, a ligand bound to a GPI-anchored form of CD4 was localized to caveolae and was internalized at a relatively slow rate (initial rate of 0.7% per min) into endosomes (Keller et al., 1992). However, the capability of caveolae to be internalized has been questioned (Bundgaard, 1983; Anderson, 1993; Van Deurs et al., 1993) based on the finding that the GPI-anchored folate receptor and VIP21/caveolin could not be observed within endosomal elements (Rothberg et al., 1990*b*, 1992) and from serial section analysis of caveolae in endothelial cells where the vast majority of caveolae, if not all, were shown to be connected to the cell surface (Bundgaard et al., 1983). Nevertheless, these studies cannot rule out a small number of asnychronous budding events which would be difficult to detect if the generated vesicles rapidly fuse with another membrane, for example, with the early endosome. Assuming that all the AP internalized in the present study in the absence of OA is through caveolae and that each budded caveola would have a lifetime of 1 min, we might expect approximately one internal caveola profile to be observed per 20 A431 cell profiles. The lifetime of a budded caveola could actually be much shorter than this. It should be noted that Tran et al. (1987) used an incubation temperature of 22°C which may have slowed down this process allowing the visualization of the intermediates. The present study is certainly consistent with the view that caveolae are capable of detachment from the cell surface at least under certain experimental conditions.

The use of an enzymatic assay allowed us to differentiate between internal and surface caveolae and to rapidly test other reagents to determine their effect on the removal of caveolae. Interestingly, staurosporine, and CytD which inhibited the OA-induced internalization of caveolae, also prevented the small decrease in surface AP activity which occurred in the absence of OA. The slow rate of AP uptake under these conditions is in the same range as that observed for CT-gold and for GPI-anchored CD4 (Tran et al., 1987; Keller et al., 1992). Further work will be required to ascertain whether the low rate of surface AP decrease observed in the present study actually corresponds to caveolar budding rather than another membrane uptake process with similar characteristics. We occasionally observed internal caveolar profiles labeled with CT-B-gold but many such profiles in serial sections were attached to groups of caveolae, narrow tubules, or multivesicular endosomal structures. We do not know whether the tubular elements are parts of the plasma membrane which are internalized together with the caveolae or endosomal structures to which the caveolae rapidly fuse. However, consistent with previous studies it appears that markers present in caveolae are transferred to endosomes as labeling of the latter was increased upon OA treatment. In this respect it is interesting to note that detergent-insoluble complexes enriched in caveolar components were recently shown to contain rab5 (Lisanti et al., 1994*b*) postulated to be involved in coated vesicle-early endosome fusion (Bucci et al., 1992). At present we have no evidence that caveolae play a role in the internalization of GPI-anchored proteins under physiological conditions. Consis-

Published December 1, 1994

tent with the results of Mayor et al. (1994) AP was only enriched in caveolae after antibody-induced crosslinking. In the absence of antibody binding, OA treatment caused a decrease in surface-attached caveolae as judged morphologically without significantly affecting the fraction of AP on the cell surface consistent with the view that under these conditions AP is not concentrated within caveolae.

Our results suggest that the actin cytoskeleton may play a role in the internalization of caveolae. An interaction of the actin cytoskeleton with caveolae has been suggested from morphological studies (Willingham et al., 1981; Izumi et al., 1988). In addition, recent studies using detergents to enrich for possible caveolar components showed the presence of actin, gelsolin, and annexin II in these fractions (Lisanti et al., 1994*b*). It should now be possible to examine the possible role of these and other actin binding proteins in the redistribution of caveolae induced by OA. The dependence of the internalization process on actin filaments suggests a possible similarity to the pathway of endocytosis in yeast. Actin and fimbrin have both been shown to be involved in the initial internalization steps of the alpha factor receptor (Kubler and Riezman, 1993). In addition, morphological studies showed that actin and actin-binding proteins are clustered around finger-like invaginations of the yeast plasma membrane (Mulholland et al., 1994). Cortical actin patches were observed to be associated with the cell surface via these invaginations. Other internalization pathways which are dependent on actin have been described in mammalian cells. Uptake from the apical surface of epithelial cells was reduced by CytD but this appeared to reflect inhibition of internalization through clathrin-coated pits (Gottlieb et al., 1993). Uptake via a non–clathrin-dependent pathway in Vero cells was also shown to be blocked by CytD (Sandvig and van Deurs, 1990).

The dramatic effects of OA on the surface caveolae as detected biochemically suggested that we might be able to detect some redistribution of the caveolar marker VIP21/caveolin. Although initial immunofluorescence studies did not show a great effect of OA on the pattern of VIP21/caveolin labeling, to our surprise we noticed a dramatic change in the VIP21/caveolin distribution if cells were treated with OA in the presence of a hypertonic medium. The labeling completely redistributed from the periphery to the perinuclear area of the cell. This process was reversible (in the same medium) and did not affect cell viability. Agents shown to block the internalization of AP measured biochemically (e.g., CytD and staurosporine) also blocked the redistribution of VIP21/caveolin in the hypertonic medium. A striking feature of the OA treatment was the formation of clusters of caveolae at early times after OA treatment. Formation of these clusters was blocked by CytD. The caveolar clusters consist of discrete 60-nm buds attached to either a central vacuole or to long tubules. The clusters are not an artifact of OA treatment as they are also observed in untreated A431 cells (see Parton, 1994, and Fig. 6 this study). Complex arrangements of caveolae, termed rosettes, have been extensively described in adipocytes where they were postulated to play a role in the uptake of lipid precursors or in insulin action (Williamson, 1964; Jarrett and Smith, 1975; Novikoff et al., 1980). Surface caveolar markers appeared within these VIP21/caveolin-positive clusters and accumulated in the center of the cell in a microtubule-dependent step. Why should hypertonic medium cause this specific effect when combined with OA treatment? Our preliminary results suggest that the amount of CT-B–gold reaching endosomes is lower after OA treatment in the hypertonic medium than in normal medium. Hypertonic medium might therefore disrupt the interaction of caveolae with endosomes, prevent VIP21/caveolin recycling back to the cell periphery, and cause caveolar markers to be trapped in the caveolar clusters. Although no endosomal or Golgi markers were detected in the caveolar clusters formed in the hypertonic medium it is possible that caveolae interact with domains of these organelles and that their centralization is a secondary effect of this interaction. It should be noted that cholera toxin has been detected in endosomes (Tran et al., 1987) and in Golgi elements (Joseph et al., 1978, 1979) under physiological conditions. Whatever the cause, this specific interaction with microtubules must reflect some physiological process. In addition, this procedure provides a useful tool to accumulate large numbers of caveolae in the cell and so facilitate immunolabeling studies.

While our results suggest a role for phosphorylation in regulating caveolae dynamics, the nature of the kinases and their targets are unknown. Previous work showed that OA induced a mitotic-like state in cultured cells (Lucocq et al., 1991). Interestingly, we have observed VIP21/caveolin labeling associated with caveolae-like profiles close to the spindle poles of mitotic A431 and MDCK cells (Parton, R. G., and B. Joggerst, results not shown). The level of phosphorylation of many different cellular proteins and the activity of several cellular kinases will be increased during OA treatment (Cohen et al., 1990). These kinases will also be inhibited by the general kinase inhibitor staurosporine. Our results suggest that the observed effects are not mediated by protein kinase C. VIP21/caveolin, one of the major caveolar proteins, was first identified as a substrate for tyrosine phosphorylation by v-src (Glenney, 1989; Glenney and Zokas, 1989) and has shown to be phosphorylated in vitro on both serine/threonine and tyrosine (Sargiacomo et al., 1993). However, preliminary experiments suggest that OA treatment does not significantly increase the phosphorylation of VIP21/caveolin in MDCK cells (Fra, A., P. Dupree, K. Simons, R. G. Parton, results not shown). We are now trying to identify other caveolar components which could be hyperphosphorylated during OA treatment.

In conclusion, we have shown that internalization of caveolae may be a regulated process. Increased phosphorylation due to phosphatase inhibition induces removal of caveolae from the surface whereas decreased kinase activity inhibits the internalization process. Although OA caused an almost complete removal of caveolae from the surface, we envisage that physiological stimuli may cause budding of small groups or individual caveolae. This may be modulated by the state of the actin cytoskeleton which is also subject to regulation. What might be the physiological role of caveolar internalization? One possibility is that this represents a highly regulatable endocytic mechanism for membrane-bound proteins. Their small volume (approximately one fifth that of a clathrin-coated vesicle) would mean that fluid uptake by caveolae may be minimal. Alternatively, this pathway might allow the accessibility of signaling molecules present in caveolae to be modulated. One striking feature of caveolae is their high concentration of calcium-regulating molecules

(Fujimoto, 1993; Fujimoto et al., 1993). Closure of caveolae, induced by phosphorylation, might be combined with opening of calcium channels in response to an intracellular messenger. A discrete amount of calcium (contained within the uniformly-sized budded caveola) would then enter the cell. Due to the enrichment of gangliosides in caveolae, the lipid-bound sialic acids could locally concentrate calcium at these sites (Maggio, 1994). Whatever the role of the caveolae internalization described here, these assays should allow detailed study of caveolar dynamics and the role of phosphorylation in this process. In addition, the possibility to remove caveolae from the surface and to cluster them in discrete areas of the cell should facilitate the study of caveolar functions and allow localization of further caveolar components.

We are grateful to Sigrun Brendel for excellent technical assistance. We would also like to thank Paul Dupree, Anna Fra, and David Critchley for providing antibodies; Sanjay Pimplikar for sharing reagents; and Paul Dupree, Anna Fra, Gareth Griffiths, Jean Gruenberg, Sanjay Pimplikar, Sigrid Reinsch, and Marino Zerial for many helpful discussions.

Received for publication 21 March 1994 and in revised form 1 September 1994.

References

Anderson, R. G. W. 1993. Potocytosis of small molecules and ions by caveolae. *Trends Cell Biol.* 3:69–72.

Anderson, R. G. W., B. A. Kamen, K. G. Rothberg, and S. W. Lacey. 1992. Potocytosis: sequestration and transport of small molecules by caveolae. *Science (Wash. DC).* 255:410–411.

Birn, H., J. Selhub, and E. I. Christensen. 1993. Internalization and intracellular transport of folate-binding protein in rat kidney proximal tubule. *Am. J. Physiol.* 264:302–310.

Bradford, M. M. 1976. A rapid sensitive method for the quantitation of microgram quantities of protein utilizing the principle of protein-dye binding. *Anal. Biochem.* 72:248–254.

Bucci, C., R. G. Parton, I. Mather, H. Stunnenberg, K. Simons, B. Hoflack, and M. Zerial. 1992. The small GTPase rab5 functions as a regulatory factor in the early endocytic pathway. *Cell.* 70:715–728.

Bundgaard, M. 1983. Vesicular transport in capillary endothelium: does it occur? *Fed. Proc.* 42:2425–2430.

Bundgaard, M., P. Hagman, and C. Crone. 1983. The three-dimensional organization of plasmalemmal vesicular profiles in the endothelium of rat heart capillaries. *Microvasc. Res.* 25:358–368.

Carpentier, J.-L., F. Sawano, D. Geiger, P. Gorden, A. Perrelet, and L. Orci. 1989. Potassium depletion and hypertonic medium reduce "non-coated" and clathrin-coated pit formation, as well as endocytosis through these two gates. *J. Cell Physiol.* 138:519–526.

Chang, W.-J., K. G. Rothberg, A. Kamen, and R. G. W. Anderson. 1992. Lowering of the cholesterol content of MA104 cells inhibits receptor-mediated transport of folate. *J. Cell Biol.* 118:63–69.

Chavrier, P., R. G. Parton, H. P. Hauri, K. Simons, and M. Zerial. 1990. Localization of low molecular weight GTP binding proteins to exocytic and endocytic compartments. *Cell.* 62:317–329.

Cohen, P., C. F. B. Holmes, and Y. Tsukitani. 1990. Okadaic acid; a new probe for the study of cellular regulation. *Trends Biochem. Sci.* 15:98–102.

Dupree, P., R. G. Parton, G. Raposo, T. V. Kurzchalia, and K. Simons. 1993. Caveolae and sorting in the trans-Golgi-network of epithelial cells. *EMBO (Eur. Mol. Biol. Organ.) J.* 12:1597–1605.

Fiedler, K., R. G. Parton, R. Kellner, T. Etzold, and K. Simons. 1994. VIP-36, a novel component of glycolipid rafts and exocytic carrier vesicles in epithelial cells. *EMBO (Eur. Mol. Biol. Organ.) J.* 13:1729–1740.

Fujimoto, T. 1993. Calcium pump of the plasma membrane is localized in caveolae. *J. Cell Biol.* 120:1147–1157.

Fujimoto, T., S. Nakade, A. Miyawaki, K. Mikoshiba, and K. Ogawa. 1993. Localization of inositol 1,4,5,-triphosphate receptor-like protein in plasmalemmal caveolae. *J. Cell Biol.* 119:1507–1513.

Ghitescu, L., A. Fixman, M. Simionescu, and N. Simionescu. 1986. Specific binding sites for albumin restricted to plasmalemmal vesicles of continuous capillary endothelium: receptor-mediated transcytosis. *J. Cell Biol.* 102: 1304–1311.

Glenney, J. R. 1989. Tyrosine phosphorylation of a 22-kDa protein is correlated with phosphorylation by Rous sarcoma virus. *J. Biol. Chem.* 264: 20163–20166.

Glenney, J. R., and L. Zokas. 1989. Novel tyrosine kinase substrate from Rous sarcoma virus-transformed cells are present in the membrane skeleton. *J. Cell Biol.* 108:2401–2408.

Gottlieb, T. A., I. E. Ivanov, M. Adesnik, and D. D. Sabatini. 1993. Actin microfilaments play a critical role in endocytosis at the apical but not the basolateral surface of polarized epithelial cells. *J. Cell Biol.* 120:695–710.

Griffiths, G. 1993. Fine Structure Immunocytochemistry. Springer-Verlag, Berlin-Heidelberg. 181–183.

Hjelle, J. T., E. I. Christensen, F. A. Carone, and J. Selhub. 1991. Cell fractionation and electron microscope studies of kidney folate-binding protein. *Am. J. Physiol.* 260:338–346.

Izumi, T., Y. Shibata, and T. Yamamoto. 1988. Striped structures on the cytoplasmic surface membranes of the endothelial vesicles of the rat aorta revealed by quick-freeze, deep-etching replicas. *Anat. Rec.* 220:225–232.

Jarrett, L., and R. M. Smith. 1975. Ultrastructural localization of insulin receptors on adipocytes. *Proc. Natl. Acad. Sci. USA.* 72:3256–3530.

Joseph, K. C., S. U. Kim, A. Stieber, and N. K. Gonatas. 1978. Endocytosis of cholera toxin into neuronal GERL. *Proc. Natl. Acad. Sci. USA.* 75: 2815–2819.

Joseph, K. C., A. Stieber, and N. K. Gonatas. 1979. Endocytosis of cholera toxin in GERL-like structures of murine neuroblastoma cells pretreated with GM1 ganglioside. *J. Cell Biol.* 81:543–554.

Keller, G. A., M. W. Siegel, and I. W. Caras. 1992. Endocytosis of glycophospholipid-anchored and transmembrane forms of CD4 by different endocytic pathways. *EMBO (Eur. Mol. Biol. Organ.) J.* 11:863–874.

Kobayashi, T., and J. M. Robinson. 1991. A novel intracellular compartment with unusual secretory properties in human neutrophils. *J. Cell Biol.* 113:743–756.

Kubler, E., and H. Riezman. 1993. Actin and fimbrin are required for the initial internalization step of endocytosis in yeast. *EMBO (Eur. Mol. Biol. Organ.) J.* 12:2855–2862.

Kurzchalia, T. V., P. Dupree, and S. Monier. 1994. VIP21-Caveolin, a protein of the trans-Golgi network and caveolae. *FEBS (Fed. Eur. Biochem. Soc.) Lett.* 346:88–91.

Lisanti, M. P., P. E. Scherer, Z.-L. Tang, and M. Sargiacomo. 1994*a*. Caveolae, caveolin and caveolin-rich membrane domains: a signalling hypothesis. *Trends Cell Biol.* 4:231–235.

Lisanti, M. P., P. E. Scherer, J. Vidugiriene, Z.-L. Tang, A. Hermanowski-Vosatka, Ya-Huei Tu, R. F. Cook, and M. Sargiacomo. 1994*b*. Characterization of caveolin-rich membrane domains isolated from an endothelial-rich source: implications for human disease. *J. Cell Biol.* 126:111–126.

Lucocq, J. 1992. Mimicking mitotic Golgi assembly using okadaic acid. *J. Cell Sci.* 103:875–880.

Lucocq, J. M., E. G. Berger, and G. Warren. 1989. Mitotic Golgi fragments in HeLa cells and their role in the reassembly pathway. *J. Cell Biol.* 109:463–474.

Lucocq, J., G. Warren, and J. Pryde. 1991. Okadaic acid induces Golgi apparatus fragmentation and arrest of intracellular transport. *J. Cell Sci.* 100: 753–759.

Maggio, B. 1994. The surface behaviour of glycosphingolipids in biomembranes: a new frontier of molecular ecology. *Prog. Biophys. Mol. Biol.* 62:55–117.

Mayor, S., K. Rothberg, and F. Maxfield. 1994. Sequestration of GPI-anchored proteins in caveolae triggered by crosslinking. *Science (Wash. DC).* 264: 1948–1951.

Milici, A. J., N. W. Watrous, H. Stukenbrok, and G. E. Palade. 1987. Transcytosis of albumin in capillary endothelium. *J. Cell Biol.* 105:2603–2612.

Montesano, R., J. Roth, A. Robert, and L. Orci. 1982. Non-coated membrane invaginations are involved in binding and internalization of cholera and tetanus toxins. *Nature (Lond.).* 296:651–653.

Mulholland, J., D. Preuss, A. Moon, A. Wong, D. Drubin, and D. Botstein. 1994. Ultrastructure of the yeast actin cytoskeleton and its association with the yeast cytoskeleton. *J. Cell Biol.* 125:381–389.

Novikoff, A. B., P. M. Novikoff, O. M. Rosen, and C. S. Rubin. 1980. Organelle relationships in cultured 3T3-L1 preadipocytes. *J. Cell Biol.* 87:180–196.

Parton, R. G. 1994. Ultrastructural localization of gangliosides; GM1 is concentrated in caveolae. *J. Histochem. Cytochem.* 42:155–166.

Parton, R. G., C. D. Ockleford, and D. R. Critchley. 1988. Tetanus toxin binding to mouse spinal cord cells: an evaluation of the role of gangliosides in toxin internalization. *Brain Res.* 475:118–127.

Parton, R. G., P. Schrotz, C. Bucci, and J. Greunberg. 1992. Plasticity of early endosomes. *J. Cell Sci.* 103:335–348.

Peters, K. R., W. W. Carley, and G. E. Palade. 1985. Endothelial plasmalemmal vesicles have a characteristic striped bipolar surface structure. *J. Cell Biol.* 101:2233–2238.

Raposo, G., I. Dunia, C. Delavier-Klutchko, S. Kaveri, A. D. Strosberg, and E. L. Benedetti. 1989. Internalization of β-adrenergic receptor in A431 cells involves non-coated vesicles. *Eur. J. Cell Biol.* 50:340–352.

Rothberg, K., Y. Ying, B. A. Kamen, and R. G. W. Anderson. 1990*a*. Cholesterol controls the clustering of the glycophospholipid-anchored membrane receptor for 5-methyltetrahydrofolate. *J. Cell Biol.* 111:2931–2938.

Rothberg, K., Y. Ying, J. F. Kolhouse, B. A. Kamen, and R. G. W. Anderson. 1990*b*. The glycophospholipid-linked folate receptor internalizes folate

without entering the clathrin-coated pit endocytic pathway. *J. Cell Biol.* 110:637–649.

Rothberg, K., J. E. Heuser, W. C. Donzell, Y.-S. Ying, J. R. Glenney, and R. G. W. Anderson. 1992. Caveolin, a protein component of caveolae membrane coats. *Cell.* 68:673–682.

Sandvig, K., and B. van Deurs. 1990. Selective modulation of the endocytic uptake of ricin and fluid phase markers without alteration in transferrin endocytosis. *J. Biol. Chem.* 265:6382–6388.

Sargiacomo, M., M. Sudol, Z. Tang, and M. P. Lisanti. 1993. Signal transducing molecules and GPI-linked proteins form a caveolin-rich insoluble complex in MDCK cells. *J. Cell Biol.* 122:789–807.

Severs, N. J. 1988. Caveolae: static inpocketings of the plasma membrane, dynamic vesicles or plain artifact? *J. Cell Sci.* 90:341–348.

Simionescu, M., and N. Simionescu. 1991. Endothelial transport of macromolecules: Transcytosis and endocytosis. *Cell Biol. Rev.* 25:1–80.

Smart, E. J., D. Foster, Y.-S. Ying, B. A. Kamen, and R. G. W. Anderson. 1993. Protein kinase C activators inhibit receptor-mediated potocytosis by preventing internalization of caveolae. *J. Cell Biol.* 124:307–313.

Tran, D., J.-L. Carpentier, F. Sawano, P. Gorden, and L. Orci. 1987. Ligands internalized through coated or non-coated invaginations follow a common intracellular pathway. *Proc. Natl. Acad. Sci. USA.* 84:7957–7961.

Turek, J. J., C. P. Leamon, and P. S. Low. 1993. Endocytosis of folate-protein conjugates: ultrastructural localization in KB cells. *J. Cell Sci.* 106:423–430.

Van Deurs, B., P. K. Holm, K. Sandvig, and S. H. Hansen. 1993. Are caveolae involved in endocytosis? *Trends Cell Biol.* 3:249–251.

Williamson, J. R. 1964. Adipose tissue. Morphological changes associated with mobilization. *J. Cell Biol.* 20:57–74.

Willingham, M. C., S. S. Yamada, P. J. A. Davies, A. V. Rutherford, M. G. Gallo, and I. Pastan. 1981. Intracellular localization of actin in cultured fibroblasts by electron microscopic immunocytochemistry. *J. Histochem. Cytochem.* 29:17–37.

Ying, Y.-S., R. G. W. Anderson, and K. G. Rothberg. 1992. Each caveola contains multiple glycosyl-phosphatidylinositol anchored membrane proteins. *Cold Spring Harbor Symp. Quant. Biol.* 57:593–604.